

An Improved Satellite Image Enhancement based Adaptive Bilateral Filter

Almukhtar Ahmed¹

Electrical & Electronics Dept., Faculty of Engineering Sabratha,
Sabratha University, Sabratha- Libya

Abstract:- The drawback is the loss of High Frequency Content in Resolution Enhancement Systems, which leads to a blur. For RE of satellite pictures, a wavelet domain technique based on the two-tree complex wavelet transform (DT-CWT) and Adaptive Bilateral Filter (ABF) is presented. The simulation results demonstrate how the new method improves the conventional one.

Keywords:- Wavelet, ABF Filter, MATLAB Simulation.

I. INTRODUCTION

The Fourier transform's weakness that it is difficult to gather the temporal information at which the various frequency components occur led to the development of the wavelet transform [10,13]. Only up to a certain point is simultaneous temporal and frequency localisation possible using the wavelet transform. Using wavelets, which have finite duration and energy, the wavelet transform analyzes the signals [1,3]. A novel representation of the signals created by the wavelet allows for the localisation of both time and frequency. As a result, wavelet transform may be used to analyze non-stationary data. Depending on our needs, we may choose from a range of wavelets for signal processing. Continuous wavelet transformations (CWTS) and discrete wavelet transforms (DWTS) are two different types of wavelet transform. For analyzing and manipulating digital images at various resolutions, DWT is a superb tool. because it offers a strong insight into the spatial and frequency aspects of the image. Four fundamental functions that have reparability, scalability, translatability, multiresolution, compatibility, and orthogonibility are what define the 2DWT. It has one 2-D.

➤ *Scaling Function:*

$$\Phi(x,y) = \Phi(x) \Phi(y) \dots \dots \dots (1)$$

➤ *And three Separable 2-D Wavelet Functions:*

- *Horizontal Wavelet Fun.*

$$\varphi_H(x,y) = \varphi(x) \varphi(y) \dots \dots \dots (2)$$

- *Vertical Wavelet fun.*

$$\varphi_V(x,y) = \varphi(y) \varphi(x) \dots \dots \dots (3)$$

- *Diagonal Wavelet Fun.*

$$\varphi_D(x,y) = \varphi(x) \varphi(y) \dots \dots \dots (4)$$

The input image's estimated low frequency information is captured by the scaling function, while horizontal features are captured by the wavelet function $H(x,y)$ [4,6]. The diagonal wavelet function $D(x,y) = \varphi(x) \varphi(y)$ captures the image's diagonal features whereas the vertical wavelet function $V(x,y)$ captures the image's vertical details. So, the wavelet functions capture the bandpass or high pass frequencies in the input picture, whereas the scaling function catches low frequency [1,2]. While $\varphi(x)$ and $\varphi(y)$ are 1-D wavelet functions, $\Phi(x)$ and $\Phi(y)$ are 1-D scaling functions. These scaling and wavelet functions can be appropriately scaled and translated as shown by

$$\Phi_{j,k}(x) = 2^{j/2} \Phi(2^j x - k) \dots \dots \dots (5)$$

$$\varphi_{j,k}(x) = 2^{j/2} \varphi(2^j x - k) \dots \dots \dots (6)$$

The basis functions' location is determined by the integer k ; their breadth and weight are determined by the binary scaling 2^j ; and their amplitude is controlled by $2^{j/2}$. The following equations can be used as representations for the breakdown and reconstruction of a digital picture using DWT:

$$\Phi(x) = \sum_n h_\Phi(n) \sqrt{2} \Phi(2x-1) \dots \dots \dots (7)$$

$$\varphi(x) = \sum_n h_\varphi(n) \sqrt{2} \Phi(2x-1) \dots \dots \dots (8)$$

Where $h_\Phi(n)$ and $h_\varphi(n)$ are the scaling and wavelet vectors.

II. IMAGE ENHANCEMENT

Picture enhancement is one of the primary steps in image processing. As the name implies, this approach alters the original picture such that the final product is better suited for particular purposes than the original. Enhancing images is solely a subjective processing method [7,9]. By using the available data, it only raises the photographs' perceived quality. There are two areas where image improvement may be done:

- *The Spatial Domain.*
- *The Frequency Domain.*

There are two types of spatial processing: point processing and neighborhood processing. In point processing, each pixel is taken into account and modified as needed. Some typical point Digital negative, contrast stretching, thresholding, bit plane slicing, and dynamic

range compression are a few processing methods. When doing neighborhood processing, we take into account a pixel and its nearby pixels.

III. ABF FILTER

In (1) and (2), the suggested ABF and its impulse response are depicted, respectively.

$$f[m, n] = h[m, n; k, l]g[k, l].....(9)$$

Where $g[m, n]$ is the degraded picture, $f[m, n]$ is the restored image, and $h[m, n; k, l]$ is the response at $[m, n]$ to an impulse at $[k, l]$.

$$h[m,n;m_0,n_0]=I(\Omega_{m_0,n_0})r^{-1}m_0,n_0e^{-(m-m_0)^2+(n-n_0)^2}2\sigma d^2*e^{-12} g[m,n]-g[m_0,n_0]-\zeta[m_0,n_0]\sigma r[m_0,n_0]^2.....(10)$$

Where $[m_0, n_0]$ is the center pixel of the window, $\Omega_{m_0,n_0} = \{[m, n]:[m, n] \in [m_0 - N, m_0 + N] \times [n_0 - N, n_0 + N]\}$, $I(\cdot)$ denotes the indicator function, and r_{m_0,n_0} normalizes the volume under the filter to unity[3,8]. Compared to a normal two-sided filter includes two important changes to ABF: First, an offset ζ is added to the interval filter. Second, both ζ and the width of the area filter σr in ABF is locally adaptive. If $\zeta = 0$ and σr is fixed, the ABF degenerates into a conventional bilateral filter [6,11]. Fixed low pass for domain filter A Gaussian filter with $\sigma d = 1.0$ is applied in ABF. The combination of locally adaptive ζ and σr makes the bipartite filters into a much more efficient filter capable of both smoothing and sharpening. In addition, it makes the image sharper raising the edges' gradient. We must comprehend the functions of ζ and σr in ABF in order to comprehend how it operates. The area filter may be thought of as a one-dimensional image histogram processing.

In a traditional bilateral filter, the distance filter resides in the gray value of the current in the histogram pixels and scrolls as the pixel values decrease value of the central pixel[13]. Adding move ζ to the interval filter, we can now change the value area filter on the histogram. As before, let Ω_{m_0,n_0} a set of pixels in a $(2N + 1) \times (2N + 1)$ pixel window centered at $[m_0, n_0]$. Let there be MIN, MAX and MEAN operations to take the data's lowest, maximum, and average values, expressed in Ω_{m_0, n_0} units. Allow Δ_{m_0, n_0} to equal $g[m_0, n_0] - \text{MEAN}(m_0, n_0)$. We greatly improve the bilateral filter by jointly maximizing the two parameters, σr and ζ , and making them adaptable. a filter that is effective and functional. To utilize a spatial Gaussian filter with two-way filtering, we can relocate the pixel filter region to $\text{MEAN}(m_0,n_0)$ and/or use a high value of Σr . Depending on whether the region to sharpen the pixel filters is above or below the center of the edge slope, we may change it from $\text{MEAN}(m_0,n_0)$ to $\text{MAX}(m_0,n_0)$ or $\text{MIN}(m_0,n_0)$. In parallel, we precisely lower σr . When r is small, the distance filter takes precedence over the bilateral filter and effectively pushes or lifts pixels that are on the edge slope..

IV. ADJUSTMENT OF ABF PARAMETERS

➤ *Mean Square Error*

The mean squared error (MSE) of an estimator in statistics is the average of the squares of the "errors," or the difference between the estimator and what is estimated[11]. The expected value of the quadratic or squared error loss corresponds to the risk function MSE. The gap might be attributed to randomness or the estimator's lack for information that would have led to a more precise estimate. Since the MSE represents the second moment of the error (around the origin), it includes both the variance and bias of the estimator. For an unbiased estimator, the MSE equals the estimator's variance. The variance and square of the quantity being assessed are used as the units of measurement by MSE. By calculating the square root of the MSE, one may derive the root-mean-square error (RMSE) or root-mean-square deviation (RMSD), which has the same units as the quantity being assessed. The square root of the variance, sometimes referred to as the standard deviation, is the RMSE for an unbiased estimator.

$$MSE = \frac{1}{N \times M} \sum_{i=0}^{N-1} \sum_{j=0}^{M-1} [X(i, j) - Y(i, j)]^2(11)$$

MSE values can be used to make comparisons. The MSEs of two or more statistical models can be used to examine how well they explain a certain collection of observations: The best prediction is an unbiased estimator (derived from a statistical model) with the least variance among all unbiased estimators. This estimator is known as the best unbiased estimator or MVUE (Minimum Variance Unbiased Estimator) since it minimizes variation.

➤ *Peak Signal-to-Noise Ratio*

Peak signal-to-noise ratio (PSNR), which is occasionally abbreviated, is an engineering term for comparing the maximum possible intensity of a signal to the influence of corrupting noise that degrades the signal's representation of its integrity. Because many signals have a significant dynamic range, PSNR is frequently expressed using a logarithmic decibel scale. The reconstruction quality of lossless compression codecs (such as image compression)

is most frequently assessed using PSNR. In this instance, the original data is the signal, while the mistake brought on by compression is the noise[3]. PSNR simulates the human experience of reconstruction quality by comparing compression codecs. Although a greater PSNR often suggests a higher-quality reconstruction, this may not always be the case. This measure must only be used to compare the outcomes of the same codec (or codec type) and material, thus you must be extremely careful how you define its scope[5]. Peak signal-to-noise ratio, often abbreviated PSNR, is an engineering term for the ratio of the highest conceivable signal power to the noise-cancellation power ratio, which affects the persistence of that description. Because many signals have exceptionally wide individual ranges, PSNR is typically reported down to a logarithmic decibel scale. PSNR is often used to measure the playback behavior of lossy compression codecs (eg image compression)[10]. The sign of this situation is the first information, and the confusion is an error caused by pressure. Although PSNR differs from a compression codec, it is an estimate of the reproduction quality of a human impression[8]. While a higher PSNR generally indicates a higher redo, sometimes it may not. One must be very careful about the legality of this measurement; it is only decisive when considering the results of an equivalent codec (or codec type) and the same subject.

$$\begin{aligned}
 PSNR &= 10 \cdot \log_{10} \left(\frac{MAX_I^2}{MSE} \right) \\
 &= 20 \cdot \log_{10} \left(\frac{MAX_I}{\sqrt{MSE}} \right) \\
 &= 20 \cdot \log_{10} (MAX_I) - 10 \cdot \log_{10} (MSE) \dots \dots \dots (12)
 \end{aligned}$$

Here, MAXI stands for the highest pixel value that the picture may contain. It is 255 if the pixels are represented with 8 bits per sample. The MAXI is 2B-1 if the samples are represented using linear PCM at B bits per sample. Using three RGB values per pixel, color pictures, Similar to how PSNR is defined, MSE is defined as the total of all the squared value differences divided by the picture size and three. The PSNR for each channel in the new color space is given for color pictures instead after the image has been converted to a different color space.

V. RESULTS AND DISCUSSION

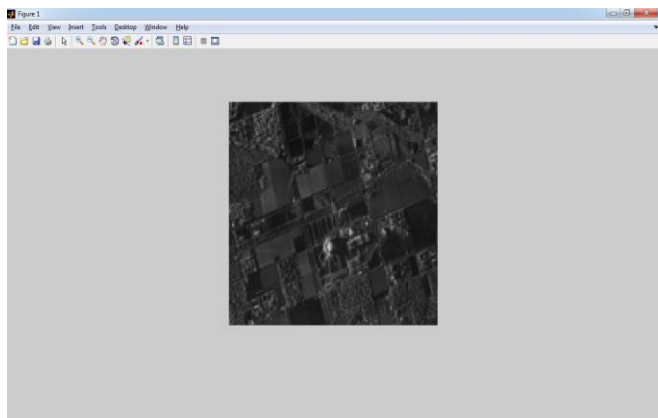


Fig 1 Input Image

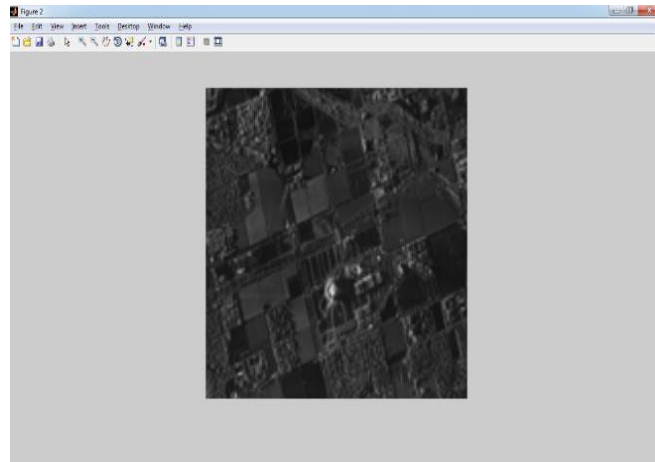


Fig 2 Output Image

Table 1 Comparison of Current and Proposed Satellite Image Techniques

Algorithm	MSE	PSNR	Time
Existing Technique	0.0286	30.8798	319.54
Proposed Technique	0.0286	30.8618	13.108

To discover the viability of the proposed method calculation over existing calculation, here we are taking a Satellite picture to go through this two cycles. In the above table, we can see that the image enhancement is successfully completed based on three factors MSE, PSNR, and time factor and was able to obtain the values 0.0286, 30.8798, and 319.54 for existing method and 0.0286, 30.8618, and 13.108 for proposed one, respectively.

VI. CONCLUSION

In order to increase the effectiveness of DTCWT, an RE method based on DTCWT and ABF filter has been suggested. The simulation results show that it produce less artifacts compared with existing method. and to additional improve the exhibition of the proposed procedure regarding MSE, PSNR, and Q-record. The simulation's outcomes demonstrate that the suggested approach performs better.

REFERENCES

- [1]. M. J. Fadili, J. Starck, and F. Murtagh, "Inpainting and zooming using sparse representations," *Comput. J.*, vol. 52, no. 1, pp. 64–79, Jan. 2009.
- [2]. H. Demirel and G. Anbarjafari, "Discrete wavelet transform-based satellite image resolution enhancement," *IEEE Trans. Geosci. Remote Sens.*, vol. 49, no. 6, pp. 1997–2004, Jun. 2011.
- [3]. H. Demirel and G. Anbarjafari, "Image resolution enhancement by using discrete and stationary wavelet decomposition," *IEEE Trans. Image Process.*, vol. 20, no. 5, pp. 1458–1460, May 2011.
- [4]. H. Demirel and G. Anbarjafari, "Satellite image resolution enhancement using complex wavelet transform," *IEEE Geosci. Remote Sens. Lett.*, vol. 7, no. 1, pp. 123–126, Jan. 2010.

- [5]. H. Demirel and G. Anbarjafari, "Image super resolution based on interpolation of wavelet domain high frequency subbands and the spatial domain input image," *ETRI J.*, vol. 32, no. 3, pp. 390–394, Jan. 2010.
- [6]. H. Zheng, A. Bouzerdoun, and S. L. Phung, "Wavelet based non-localmeans super-resolution for video sequences," in *Proc. IEEE 17th Int.Conf. Image Process.*, Hong Kong, Sep. 26–29, 2010, pp. 2817–2820.
- [7]. M. Protter, M. Elad, H. Takeda, and P. Milanfar, "Generalizing the nonlocal-means to super-resolution reconstruction," *IEEE Trans. ImageProcess.*, vol. 18, no. 1, pp. 36–51, Jan. 2009.
- [8]. J. L. Starck, F. Murtagh, and J. M. Fadili, *Sparse Image and Signal Processing: Wavelets, Curvelets, Morphological Diversity*. Cambridge, U.K.: Cambridge Univ. Press, 2010.
- [9]. C. G. Diniz et al., "DETER-B: The new amazon near real-time deforestation detection system", *IEEE J. Sel. Topics Appl. Earth Observ. Remote Sens.*, vol. 8, no. 7, pp. 3619-3628, Jul. 2015
- [10]. L. O. Pereira, C. C. Freitas, S. J. S. Sant'Anna and M. S. Reis, "ALOS/PALSAR data evaluation for land use and land cover mapping in the amazon region", *IEEE J. Sel. Topics Appl. Earth Observ. Remote Sens.*, vol. 9, no. 12, pp. 5413-5423, Dec. 2016.
- [11]. R. Pouteau and B. Stoll, "Fusion for classes in difficulty for accurate and speed tropical rainforests classification", *Proc. IEEE Int. Geosci. Remote Sens. Symp.*, pp. 740-743, 2011
- [12]. L. F. d. A. Furtado, T. S. F. Silva, P. J. F. Fernandes and E. M. L. d. M. Novo, "Land cover classification of Lago Grande de Curuai floodplain (Amazon Brazil) using multi-sensor and image fusion techniques", *Acta Amazonica*, vol. 45, pp. 195-202, 2015
- [13]. L. Pereira, C. Freitas, S. Sant'Anna, D. Lu and E. Moran, "Optical and radar data integration for land use and land cover mapping in the Brazilian Amazon", *GISci. Remote Sens.*, vol. 50, no. 3, pp. 301-321, 2013.